The Encoding/Retrieval Flip: Interactions between Memory Performance and Memory Stage and Relationship to Intrinsic Cortical Networks

Willem Huijbers[1,2,3], Aaron P. Schultz[3,4], Patrizia Vannini[1,2,3], Donald G. McLaren[1,3,4], Sarah E. Wigman[3,4], Andrew M. Ward[3,4], Trey Hedden[1,3,4], and Reisa A. Sperling[1,2,3,4]

Abstract

■ fMRI studies have linked the posteromedial cortex to episodic learning (encoding) and remembering (retrieval) processes. The posteromedial cortex is considered part of the default network and tends to deactivate during encoding but activate during retrieval, a pattern known as the encoding/retrieval flip. Yet, the exact relationship between the neural correlates of memory performance (hit/miss) and memory stage (encoding/retrieval) and the extent of overlap with intrinsic cortical networks remains to be elucidated. Using task-based fMRI, we isolated the pattern of activity associated with memory performance, memory stage, and the interaction between both. Using resting-state fMRI, we identified which intrinsic large-scale functional networks overlapped with regions showing task-induced effects. Our results demonstrated an effect of successful memory performance in regions associated with the control network and an effect of unsuccessful memory performance in the ventral attention network. We found an effect of memory retrieval in brain regions that span the default and control networks. Finally, we found an interaction between memory performance and memory stage in brain regions associated with the default network, including the posteromedial cortex, posterior parietal cortex, and parahippocampal cortex. We discuss these findings in relation to the encoding/retrieval flip. In general, the findings demonstrate that task-induced effects cut across intrinsic cortical networks. Furthermore, regions within the default network display functional dissociations, and this may have implications for the neural underpinnings of age-related memory disorders. ■

INTRODUCTION

Neuroimaging has revealed that learning (encoding) and remembering (retrieval) episodic memories are associated with distinct patterns of activity across the brain. A set of regions—overlapping the default network—tends to decrease when individuals encode information into episodic memory (Kim, 2011; Shrager, Kirwan, & Squire, 2008; Daselaar, Prince, & Cabeza, 2004; Otten & Rugg, 2001). In contrast, retrieval of episodic memories tends to increase activity in a subset of the same regions, including posterior parietal cortex (PPC) and posteromedial cortex (PMC; Hutchinson, Uncapher, & Wagner, 2009; Konishi, Wheeler, Donaldson, & Buckner, 2000; Schacter, Buckner, Koutstaal, Dale, & Rosen, 1997). Several studies have recently demonstrated overlap between these encoding-related deactivations and retrieval-related activations, a pattern known as the encoding/retrieval flip (E/R flip; Vannini et al., 2011, in press; Gilbert, Armbruster, & Panagiotidi, 2011; Huijbers, Pennartz, Cabeza, & Daselaar, 2009, 2011; Kim, Daselaar, & Cabeza, 2010; Daselaar et al., 2009). However, there has been considerable variation between studies in the exact location of the E/R flip and whether the flip occurs primarily in the default network.

A related question is whether successful (hits) versus unsuccessful (miss) memory performance has an impact on the E/R flip. The E/R flip was originally defined as an overlap between the negative encoding success effect (encoding hit < miss) and the positive retrieval success effect (retrieval hit > miss; Daselaar et al., 2009; Huijbers et al., 2009) and was observed in both PPC and PMC. This method of defining the E/R flip has the advantage of being independent from an fMRI baseline but can be influenced by differential performance across encoding and retrieval stages. Recent studies have also observed an E/R flip in the PMC using a method contrasting successful encoding and successful retrieval to baseline (Vannini et al., 2011, in press). This baseline-dependent approach could also be influenced by differential performance across memory stages but may also be affected by baseline differences between the different stages, especially when encoding and retrieval are tested in different sessions. Hence, the extent to which the E/R flip is driven by memory performance (hit/miss) versus memory stage (encoding/retrieval) remains unclear.

[1]Harvard Medical School, [2]Brigham and Women's Hospital, [3]Athinoula A. Martinos Center for Biomedical Imaging, Charlestown, MA, [4]Massachusetts General Hospital

Journal of Cognitive Neuroscience 25:7, pp. 1163–1179
doi:10.1162/jocn_a_00366

In the current study, we examine the following question: Does the E/R flip represent an interaction between memory performance (hit/miss) and memory stage (encoding/retrieval), or alternatively, is the E/R flip driven primarily by either memory stage or performance? To identify the influence of memory performance and stage on fMRI activity—and the interaction between these processes—we designed an experiment in which healthy young participants simultaneously encoded and retrieved information. The design allowed separate modeling of the main effects and statistical interactions between memory performance (hit/miss) and memory stage (encoding/retrieval). This methodological approach alleviates some of the difficulties associated with interpreting statistical interactions in fMRI, which stem from the fact that the fMRI signal is a relative measure (Gusnard & Raichle, 2001; Stark & Squire, 2001). Because activity levels can be modulated by the cognitive state of the participant (Andrews-Hanna, Reidler, Huang, & Buckner, 2010; Hayden, Smith, & Platt, 2009; Weissman, Roberts, Visscher, & Woldorff, 2006), having encoding and retrieval occur during the same run, rather than in different runs, allows a more direct comparison between the two memory stages in the context of a common baseline. Guided by earlier E/R flip studies (Vannini et al., 2011; Daselaar et al., 2009; Huijbers et al., 2009), we predicted an interaction between memory performance and stage within the parietal cortices, including the PPC and PMC. In addition, we explored main effects of memory performance and memory stage and the possibility that an interaction could also be observed in regions that have not been associated with the default network.

Our second aim was to clarify the location of task-induced effects—including the E/R flip—in relation to intrinsic cortical networks. Therefore, we acquired resting-state fMRI within the same set of participants. Recently, performance-related deactivations have been observed within regions overlapping both the ventral attention network and the default network using a working-memory task (Anticevic, Repovs, Shulman, & Barch, 2010). Furthermore, retrieval-related activations have been observed in regions overlapping both the control and default networks using an autobiographical memory task (Spreng, Stevens, Chamberlain, Gilmore, & Schacter, 2010). These findings suggest that memory performance- and memory stage-related activity may span multiple networks. Other neuroimaging studies indicate that the default network can be fractionated into multiple subnetworks (Damoiseaux, Prater, Miller, & Greicius, 2012; Leech, Kamourieh, Beckmann, & Sharp, 2011; Andrews-Hanna, Reidler, Sepulcre, Poulin, & Buckner, 2010), suggesting that memory-related effects might involve select regions within a larger network (i.e., the default network). The combination of task-induced activity and resting-state fMRI allowed us to clarify if memory-related patterns occur within individual cortical networks or across regions spanning multiple networks. The current study attempts to dissociate the neurocorrelates of memory performance, memory stage, and the interaction between both and to clarify the location of memory-related activity in relation to intrinsic large-scale cortical networks.

METHODS

Participants

Forty-five young, cognitively normal adults (28 women) aged 24.5 years (SD = 0.5 years) were recruited from the Boston area. All participants were native English speakers, had normal or corrected-to-normal vision, and were right-handed. No participant had a history of psychiatric or neurological disorders or reported taking medications that affect the CNS. Informed written consent was obtained from every participant before experimental procedures, and the study was approved by and conducted in accordance with the Partners Human Research Committee at the Brigham and Women Hospital and Massachusetts General Hospital (Boston, MA). Data from two additional participants were excluded because of data collection errors during scanning.

Experimental Paradigm

The experimental paradigm consisted of a memory task designed to acquire fMRI images both during learning (encoding) and remembering (retrieval; Figure 1). The paradigm consisted of three sessions in one visit: (1) prescan, (2) scan, and (3) postscan sessions. Across all sessions, participants observed, in total, a set of 450 faces with an emotionally neutral expression paired with fictional first names, similar as those used in Minear and Park (2004) and Sperling et al. (2001). Participants initially learned a set of face–name pairs ("novel" pairs) and subsequently identified previously seen ("old") face–name pairs, "re-paired" faces and names, and completely novel face–name pairs.

In the prescan session (outside the scanner), 150 novel face–name pairs were encoded. During this session, colored photographs of faces were presented against a black background with a fictional first name printed in white below the face (face–name pairs). Participants were explicitly told to remember the name associated with the face. Participants were asked to press a button indicating whether the name was a good "fit" for the face and another button if the name was not a good "fit" for the face. This type of judgment is known to facilitate learning and ensured that the participants attended to both the face and the name (Sperling et al., 2003). The prescan session consisted of three runs. In each run, 50 face–name pairs were shown for 3750 msec apiece with a constant 250-msec intertrial interval, during which a white crosshair was presented on the screen.

In the scan session, participants again viewed face–name pairs. Fifty percent of the face–name pairs were completely novel. Forty percent of the face–name pairs

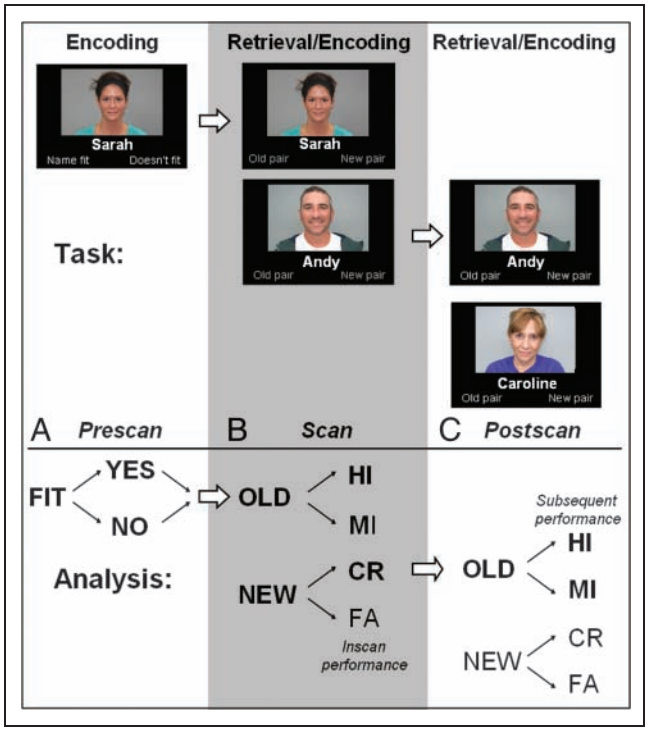

Figure 1. Task design and analysis: The experimental task involved three sessions: (A) prescan, (B) scan, and (C) postscan sessions. (A) During the prescan session, participants encoded face–name pairs and judged if the name fit the face (yes/no). This judgment had no direct consequences for the fMRI analysis. (B) During the scan session (gray column), participants retrieved and encoded face–name pairs by judging whether they had seen the exact face–name pair before (yes/no). This judgment determined if items were classified as a retrieval hit (HI), miss (MI), correct rejection (CR), or false alarm (FA) for the fMRI analysis. (C) During the postscan session, participants again retrieved and encoded face–name pairs by judging whether they had seen the exact face–name pair before (yes/no). Using the subsequent memory performance, this judgment determined if items were classified as an encoding hit (HI) or miss (MI) for the fMRI analysis. Note that only correct rejections during the scan session were used to examine the neural correlates of memory encoding (indicated by bold).

were "old," thus previously presented during the prescan session. Ten percent of the face–name pairs were "re-paired." Re-paired face–name pairs were created by re-pairing a previously seen face, presented during the prescan session, with a previously seen name. However, the face and name presented together for "re-paired" stimuli were not previously seen together. In total, the scan session consisted of retrieval of 120 old and 30 re-paired face–name pairs and encoding of 150 new face–name pairs. The few number of re-paired items allowed participants to perform 90% of the task using a recognition strategy.

Re-paired faces–name pairs were included to ensure that participants attended to both the face and the name. Participants were asked to press one button to indicate that they had seen the exact face–name pair before and a different button if they had not seen the exact face–name pair before (hence, re-paired pairs were to be assigned the same response as novel pairs). Participants were also told that they should try to learn the novel face–name pairs, as they would be tested in the postscan session. To ensure that participants were attentive and understood the instructions, detailed oral instructions were recited before each run. The scan session consisted of six runs. In each run, 50 face–name pairs were shown for 3750 msec with an intertrial interval varying between 250 and 10250 msec (average = 3300 msec), during which a white crosshair was presented on the screen. The range of the intertrial intervals and trial order was optimized using optseq2 (surfer.nmr.mgh.harvard.edu/optseq; Dale, Greve, & Burock, 1999).

In the postscan session (outside the scanner), participants conducted a task almost identical to the scan session. Again, 50% of the face–name pairs were completely novel, 40% of the face–name pairs were "old" and presented during the scan session, and 10% of the face–name pairs were "re-paired." Re-paired pairs were created by re-pairing the "novel" face–name pairs from the scan session. Participants were again asked to press a button indicating whether they had seen the exact face–name pair before. The postscan session consisted of three runs. In each run, 100 face–name pairs were shown for a maximum of 9000 msec. When a response was made, the next item appeared on the screen after a 1000-msec delay. On average, participants responded within the same time as during the scan session (see Results). This nearly self-paced timing was used to minimize the number of omissions. Note that the postscan was only used to determine the subsequent memory of novel pairs encoded inside the scanner. In total, the participants retrieved 120 old and 30 re-paired face–name pairs (from the 150 face–name pairs encoding during scanning), interspersed with an additional 150 novel face–name pairs.

All participants completed practice sessions both outside and inside of the MR scanner before the fMRI data were collected. The paradigm was designed and generated on an MacBook Pro laptop (Apple, Inc., Cupertino, CA) using the Psychophysics Toolbox (Brainard, 1997) and MATLAB (MathWorks, Natick, MA). Stimuli were projected by means of an MR-compatible goggle system (VisuaStim XGA, Resonance Technology, Inc., Los Angeles, CA). Inside the scanner, participants responded with an MRI-compatible fiber-optical keypress device with two buttons held in their right hand, and behavioral responses (accuracy and RT) were recorded by a computer using the Psychophysics Toolbox software in the scanner control room. In the pre and postscan sessions, participants directly viewed the stimuli on the Apple computer (19″-in. screen) and responded via two buttons on a USB pocket keypad (Kensington Technology Group, Redwood Shores, CA).

Imaging Acquisition

The MR images were acquired using a GE Signa 3.0-T MR system equipped with an eight-channel head coil (General Electric Company, Fairfield, CT). High-resolution

T1-weighted structural images were acquired using an accelerated 3-D inversion recovery spoiled gradient-echo sequence: 196 sagittal slices, repetition time (TR) = 6.4 msec, echo time (TE) = 2.8 msec, inversion time = 400 msec, flip angle (FA) = 11°, field of view = 256 mm, matrix = 256 × 256, resolution of 1 × 1 × 1.2 mm. Task-related BOLD fMRI data was acquired using a T2*-weighted gradient echo-planar imaging sequence. We acquired six functional runs of 180 volumes with TR = 2000 msec, TE = 30 msec, FA = 90°, and 64 × 64 matrix size. We acquired 32 oblique 3-mm-thick slices in ascending order, with a skip of 0.8, aligned parallel to the AC–PC plane. This resulted in an effective voxel size of 3 × 3 × 3.8 mm. After the experimental task, we also acquired one resting-state run of 120 volumes with TR = 3000 msec, TE = 30 msec, FA = 85°, and 64 × 64 matrix size. We acquired 47 oblique 3-mm-thick slices in interleaved order aligned parallel to the AC–PC. This resulted in an effective voxel size of 3 × 3 × 3 mm.

fMRI Preprocessing

The functional data were preprocessed and analyzed using SPM8 (Wellcome Trust Centre for Neuroimaging, UCL, London, United Kingdom: www.fil.ion.ucl.ac.uk/spm). Functional MRI data were slice time corrected, realigned, normalized to the MNI152 echo-planar imaging template, resampled to 3 × 3 × 3 mm voxels, and smoothed with an 8-mm FWHM Gaussian kernel. Resting-state fMRI data was band-pass filtered between 0.01 and 0.08 Hz, and nuisance regressors for the white matter, lateral ventricles, and global brain signals and the motion parameters plus the first derivatives of these nuisance regressors were modeled.

Task-based fMRI

For the subject-level fMRI task analysis, we used the general linear model (GLM) as implemented in SPM8. Face–name pairs were coded into one of three types: previously seen (old), not seen (new), or re-paired. Depending on the responses, these items were classified as retrieval hit, correct rejection, and re-paired hit when correct or as retrieval miss, false alarm, or re-paired miss when incorrect. The new face–name pairs were also coded depending on the postscan subsequent memory: either as encoding hit, encoding miss, or re-paired. Omissions were also coded as separate events, resulting into 11 different trial types. The onsets plus the response time for these events were convolved with the canonical hemodynamic response function to create task regressors. Additionally, the models included the motion parameters and a high-pass filter (1/128 Hz). Contrasts were created for the trial types: retrieval hit (mean number of trials = 81 ± 2.6), retrieval miss (34 ± 2.5), encoding hit (55 ± 2.8), encoding miss (51 ± 2.9). Note that encoding hit and miss were only included in the subject-level contrasts when they were initially correctly rejected inside the scanner.

For the group-level analysis, we used SPM8 in combination with in-house MATLAB scripts (GLM-Flex, Harvard Aging Brain Study, Martinos Center, MGH, Charlestown, MA, nmr.mgh.harvard.edu/harvardagingbrain/People/AaronSchultz/Aarons_Scripts). These scripts implement a standard partitioned error GLM (consistent with the method used in SPSS, R, and SAS), as opposed to the corrected pooled error approach implemented in SPM8. The partitioned error approach makes fewer assumptions regarding independence, equality of variance, and the stability of covariance patterns across voxels and, as such, is more appropriate for a multifactor repeated measures interaction test. Similar as SPM8, GLM-Flex also corrects for violations of sphericity within each factor by pooling covariance estimates across voxels. The four beta maps (encoding hit/miss, retrieval hit/miss) from each participant were entered into a second-level model with factors for task-memory performance (hit = success, miss = failure), memory stage (new = encoding, old = retrieval), and participant. The model also included the interaction between memory performance and memory stage. Whole-brain statistical analysis was thresholded at $p < .05$, FDR corrected, with an extent threshold of >5 voxels (Table 1). For the figures, the resulting t maps were projected to the cortical surface using the standard MNI to FS-average transformation as implemented in FreeSurfer 5.0 (surfer.nmr.mgh.harvard.edu/).

Resting-state fMRI

To identify the location of task-induced fMRI effects in relation to intrinsic large-scale networks, we used resting-state fMRI data gathered within the same participants immediately after the task. Using seed-based resting-state connectivity analyses, we identified six intrinsic cortical networks using the following set of seed locations listed subsequently and published by Yeo et al. (2011). Note that that visual seeds were based on previous studies (e.g., Fischl et al., 2008; see Table 1 from Yeo et al., 2011) and the motor seeds were based on a localizer task using motion of the tongue, hand, and foot (see Figure 20 from Yeo et al., 2011). The seed locations for the other four networks, control, default, dorsal, and ventral attention networks, are based on independent cluster analysis using resting data from two data sets of 500 participants and confirmed using estimates from the second data set (see Table 5 from Yeo et al., 2011). Below, we list the MNI location for these seeds in the left hemisphere (for the right hemisphere, flip the sign of the x coordinate):

1. control network: MNI (x,y,z) = (−40,50,7),(−43,−50,64),(−57,−50,−9),(−5,22,47),(−6,4,29),(−4,−76,45)

Table 1. Effects of Memory Performance

								Task-based Effects			*Resting-state Effects*					
Label	*Side*	*BA*	*t*	*Size*	*x*	*y*	*z*	P	*S*	*P × S*	*CON*	*DMN*	*DAN*	*MOT*	*VAN*	*VIS*
Effect of Successful Memory Performance (Hit > Miss)																
DLPFC	L	9/46/47	6.02	693	−48	11	35	**41.43**	**6.97**	0.36	**10.33**	*−1.71*	**3.59**	*−0.67*	**3.76**	*−5.65*
	R	9	4.81	64	42	8	29	**20.40**	**2.91**	0.58	**10.21**	*−5.40*	**8.37**	*−2.49*	**8.60**	*−3.50*
	R	47	4.67	11	33	29	−19	**21.49**	**2.91**	0.22	*−0.87*	**3.04**	*−5.96*	*−3.89*	*−2.99*	*−3.92*
	R	47	3.60	18	39	20	−7	**13.18**	**7.77**	0.19	**4.74**	*−8.48*	0.65	*−7.04*	**5.73**	*−0.84*
	R	46	4.30	34	48	29	17	**17.11**	0.02	1.01	**4.73**	**2.19**	*−0.14*	*−0.38*	**1.88**	*−4.44*
PPC	R	7/40	4.63	67	33	−64	47	**18.89**	0.17	1.18	**14.95**	0.60	**7.60**	*−5.64*	*−3.24*	*−5.33*
ACC/SMA	L	8/32	4.28	61	−6	20	47	**18.20**	**11.14**	1.11	**8.56**	*−1.75*	**1.95**	*−2.00*	**1.90**	*−5.12*
Brainstem	L		3.97	14	−6	−28	−10	**15.38**	0.62	0.43	*−2.49*	**2.41**	−2.03	*−5.60*	*−2.70*	1.78
	R		4.11	19	6	−25	−13	**16.98**	0.00	0.19	*−1.68*	**2.28**	*−1.88*	*−6.30*	*−1.86*	1.51
Visual crtx.	L	18/19	6.78	322	−27	−82	−7	**30.51**	0.91	0.56	*−4.27*	*−8.91*	0.89	*−0.11*	*−1.18*	**17.58**
	L	19	3.58	17	−27	−73	32	**15.36**	1.43	1.61	*−0.45*	*−7.12*	**10.38**	1.01	0.40	**6.15**
	R	18/19	6.09	413	36	−88	8	**34.10**	**4.55**	**10.48**	*−6.43*	*−7.79*	1.63	0.79	*−2.20*	**15.17**
	R	18	3.98	11	6	−94	14	**14.73**	**22.17**	0.89	*−2.98*	*−5.98*	*−1.10*	*−3.18*	0.52	**13.47**
Effect of Unsuccessful Memory Performance (Miss > Hit)																
Dorsal precuneus	L	7	4.52	122	−6	−52	50	**23.70**	2.28	0.03	1.60	**6.22**	**6.10**	*−1.47*	**2.15**	*−6.72*
	R	7	3.64	7	9	−58	59	**12.81**	0.12	0.12	**1.78**	*−2.38*	**12.84**	0.66	**6.62**	*−2.50*
TPJ	L	22/40/41	4.30	131	−63	−31	23	**23.27**	**7.67**	0.1	*−5.13*	*−7.74*	*−0.42*	**5.24**	**9.59**	**1.81**
	R	22/40/41	6.58	174	57	−40	29	**31.66**	**5.15**	0.84	1.14	*−9.31*	**6.91**	*−0.20*	**19.52**	*−1.07*
Lateral temp. crtx.	R	41	3.82	11	57	−25	11	**16.99**	1.64	0.45	*−4.89*	*−8.59*	*−0.22*	**7.15**	**9.69**	1.63
	R	22	3.66	13	57	−55	17	**14.73**	0.93	0.11	*−5.16*	**3.40**	*−3.40*	*−0.87*	**4.04**	*−3.94*
sPFC	L	9/10	4.64	144	−33	37	34	**30.84**	**10.00**	0.15	**2.10**	0.69	**2.34**	*−3.56*	**10.65**	*−4.28*
	R	9/10	5.59	294	27	38	38	**42.74**	0.97	0.01	**7.49**	*−1.88*	**3.74**	*−6.78*	**10.78**	*−3.24*
Post. cing. crtx.	R	31	3.84	14	15	−37	44	**15.83**	0.62	2.47	**3.06**	*−3.03*	**10.18**	*−3.50*	**12.58**	*−2.01*
Somatosensory	R	5	3.37	6	24	−46	71	**12.42**	0.42	0.35	**6.99**	0.45	*−1.03*	*−3.38*	1.11	*−3.19*
Visual crtx.	R	18	4.12	32	15	−76	2	**20.34**	**13.38**	**3.49**	*−3.70*	*−9.09*	1.59	*−0.45*	*−0.42*	**15.07**

Top demonstrates effects of successful memory performance (hit > miss); bottom, an effect of unsuccessful memory performance (miss > hit). Left column shows activated regions: BA = Brodmann's area; *t* value of task-based effect; Size = cluster size in voxels; coordinates *x*, *y*, and *z* in MNI space. Middle column shows *F* values for the 2 × 2 post hoc ANOVA for each cluster, P = memory performance (selected for by task-based analysis), S = memory stage, and P × S = interaction. Significant *F* values are indicated in **bold**. Right column shows resting-state effects. Significant *t* values are indicated in **bold**; negative values are listed in italics. crtx. = cortex; temp. = temporal; post. cing. = posterior cingulate.

2. default network: MNI (x,y,z) = (−27,23,48),(−41,−60,29),(−64,−20,−9),(−7,49,18),(−25,−32,−18),(−7,−52,26)
3. dorsal attention network: MNI$_{(x,y,z)}$ = (−22,−8,54),(−34,−38,44),(−18,−69,51),(−51,−64,−2),(−8,−63,57),(−49,3,34)
4. motor network: MNI (x,y,z) = (−41,−20,62),(−6,−26,76),(−55,−4,26)
5. ventral attention network: MNI (x,y,z) = (−31,39,30),(−54,−36,27),(−60,−59,11),(−5,15,32),(−8,−24,39),(−31,11,8)
6. visual network: MNI (x,y,z) = (−12,−67,−3),(−3,−74,23),(−16,−74,7),(−23,−91,−15),(−32,−89,−1),(−13,−100,−8)

To define each network in each participant, we computed the correlation maps using the time course from spherical seeds with a 6-mm radius based on coordinates in both the left and right hemisphere by multiplying the x MNI coordinate with −1 (Biswal, Yetkin, Haughton, & Hyde, 1995). Each correlation map was transformed to a Z score using Fisher's r-to-Z transform. Next, we masked out spherical regions with 12-mm radius to remove some of the autocorrelations immediately surrounding each seed. The resulting 12 correlation maps for each network (six for the motor network) were averaged to obtain a single map for the control network (CON), default-mode network (DMN), dorsal attention network (DAN), motor network (MOT), ventral attention network (VAN), and visual network (VIS) for each participant (Yeo et al., 2011). Note, we have labeled these networks consistent with Yeo et al. (2011), but the literature varies in the exact terminology (Smith et al., 2009; Seeley et al., 2007). For example, the ventral attention network is sometimes labeled as "salience" network or the control network, as "executive" network. Next, we conducted one-sample t tests across the participant maps to obtain group maps. The resulting t maps were projected to the cortical surface using FreeSurfer (see Figure 2D), where the group maps are displayed using a "winner takes all" approach, eliminating overlap between the six intrinsic cortical networks and assigning each voxel to the network possessing the strongest correlation to the voxel's time course. Note that these maps are shown with no threshold to demonstrate the strongest connectivity of each voxel.

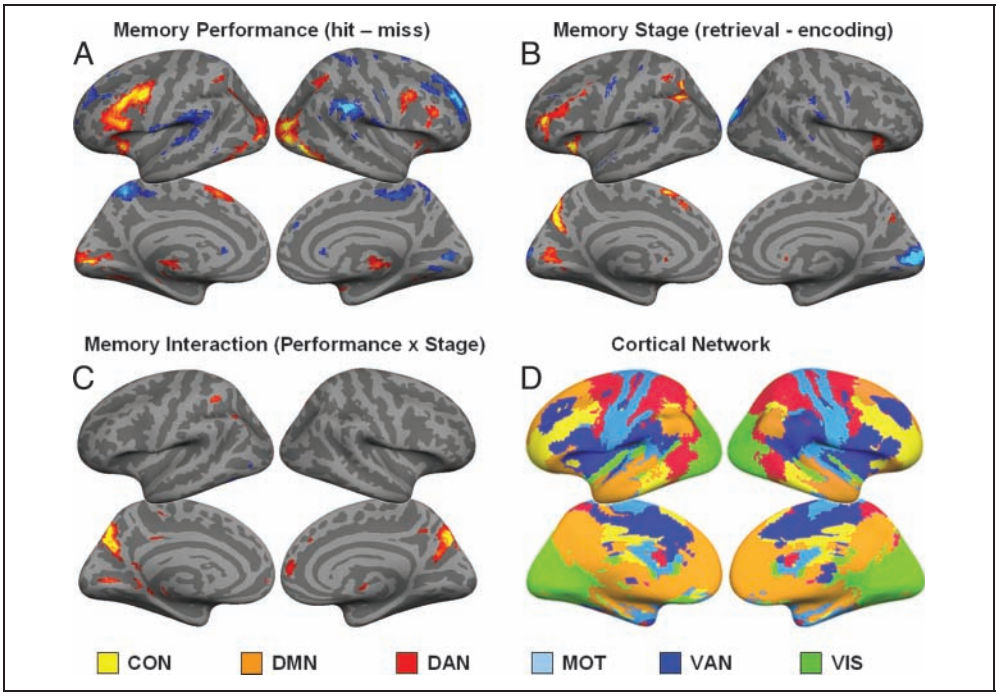

Figure 2. Statistical maps computed via a 2 × 2 ANOVA displayed at a threshold of $p < .1$, FDR corrected for visualization purposes only and projected onto the cortical surface. (A) Effects of memory performance: in red, regions showing an effect of successful memory performance (hit > miss); in blue, regions showing an effect of unsuccessful memory performance (miss > hit). (B) Effects of memory stage: in red, regions showing an effect of memory retrieval (retrieval > encoding); in blue, regions showing an effect of memory encoding (encoding > retrieval). (C) Interaction: in red, regions showing an interaction between memory performance (hit/miss) and memory stage (encoding/retrieval). (D) Resting-state networks: six cortical resting-state networks as identified by connectivity analysis based on seeds from Yeo et al. (2011). The control network (CON: yellow), default network (DMN: orange), dorsal attention network (DAN: red), motor network (MOT: baby blue), ventral attention network (VAN: dark blue), and visual network (VIS: green).

Table 2. Effects of Memory Stage

								Task-based Effects			*Resting-state Effects*				
Label	*Side*	*BA*	*t*	*Size*	*x*	*y*	*z*	*P*	*S*	*P × S*	*CON*	*DMN*	*DAN*	*MOT*	*VAN*	*VIS*
Effect of Memory Retrieval (Retrieval > Encoding)																
Ventral precuneus	L	7	5.77	142	−12	−67	29	0.01	**34.42**	**22.68**	**5.55**	**10.01**	*−1.21*	*−3.87*	*−3.57*	*−0.18*
	R	7	3.57	6	12	−70	26	0.09	**13.47**	**23.31**	0.92	**3.91**	**4.65**	0.14	0.95	**3.51**
PPC	L	7/40	5.73	201	−42	−61	44	2.37	**38.12**	**13.33**	**13.51**	**7.52**	**3.78**	*−4.23*	*−7.87*	*−7.68*
	R		3.78	15	42	−55	50	1.57	**16.32**	**3.76**	**15.52**	1.44	**3.46**	*−6.03*	*−3.29*	*−6.24*
Anterior PFC	L	9/10	5.16	91	−39	44	8	**5.20**	**34.66**	**5.40**	**11.60**	*−2.88*	**2.54**	*−1.86*	**3.51**	*−4.69*
ACC/SMA	L	32	4.97	45	−6	17	50	**11.02**	**19.16**	0.80	**11.05**	*−0.67*	**2.40**	*−3.35*	1.20	*−6.07*
	L	24	3.97	11	−6	32	35	1.61	**16.32**	1.36	**4.44**	**2.80**	*−1.81*	*−5.08*	**6.96**	*−4.93*
Premotor crtx.	L	6	4.99	114	−33	2	62	**10.06**	**31.00**	1.56	**8.43**	**6.63**	1.53	*−2.10*	*−6.37*	*−8.77*
Insula	L	13/47	5.87	64	−30	26	−10	**19.90**	**29.56**	2.26	0.46	*−0.33*	*−3.51*	*−6.33*	0.66	*−2.70*
	R	13/47	4.49	28	33	29	−4	**6.90**	**20.84**	0.36	**5.60**	*−6.39*	0.20	*−7.09*	**3.89**	*−2.04*
Caudate	L	–	7.32	135	−9	14	−4	**4.17**	**52.91**	1.58	*−1.05*	*−1.55*	*−5.01*	*−2.53*	0.20	*−3.80*
	R		5.85	98	12	11	2	**3.18**	**38.37**	1.86	1.07	*−2.49*	*−3.71*	*−3.45*	0.07	*−3.71*
Visual crtx.	L	18	4.32	60	−12	−79	2	**4.07**	**17.25**	**11.92**	*−3.20*	*−8.18*	0.50	*−1.28*	*−0.40*	**16.13**
Effect of Memory Encoding (Encoding > Retrieval)																
sPFC	L	9	4.25	15	−33	38	35	**16.95**	**22.27**	0.28	**1.91**	*−4.93*	**5.61**	*−2.04*	**11.44**	*−1.94*
Superior temp. crtx.	R	22	4.19	19	57	−58	8	1.08	**20.69**	1.25	*−2.01*	*−2.82*	**1.98**	*−1.29*	**5.05**	*−1.32*
Premotor crtx.	R	6	4.85	9	60	5	35	0.66	**18.11**	2.06	−0.52	*−5.33*	**8.14**	**7.14**	**5.44**	*−1.82*
Caudate	L	–	4.09	18	−23	11	22	0.17	**14.39**	0.93	*−1.87*	**1.97**	*−2.39*	**2.56**	*−1.93*	0.47
Visual crtx.	L/R	18	5.52	308	18	−91	14	2.42	**31.03**	1.17	*−4.46*	*−7.48*	*−1.01*	*−3.20*	*−2.09*	**16.68**

Top demonstrates effects of memory retrieval (retrieval > encoding); bottom, effect of memory encoding (encoding > retrieval). Left column shows task-based analysis: BA = Brodmann's area; *t* value of task-based effects; Size = cluster size in voxels; coordinates *x*, *y*, and *z* in MNI space. Middle column shows *F* values for the 2 × 2 post hoc ANOVA for each cluster: P = memory performance (selected for by task-based analysis), S = memory stage, P × S = interaction. Significant *F* values are indicated in **bold**. Right column shows resting-state effects. Significant *t* values are indicated in **bold**; negative values are listed in italics. crtx. = cortex; temp. = temporal.

Table 3. Interaction between Performance and Stage

	Performance (Hit/Miss) × Stage (Encoding/Retrieval)														*Post Hoc Tests*				
								Task-based Effects			*Resting-state Effects*				*ENC*	*RET*	*ENC*	*RET*	
Label	*Side*	*BA*	*t*	*Size*	*x*	*y*	*z*	*P*	*S*	*P × S*	*CON*	*DMN*	*DAN*	*MOT*	*VAN*	*VIS*	*FIX–HIT*	*HIT–FIX*	*MISS–HIT*	*HIT–MISS*
Ventral precuneus/PCC	L/R	7/31	6.36	288	−12	−70	26	0.01	**14.94**	**36.27**	**2.13**	**7.23**	1.43	*−1.26*	*−2.03*	**4.58**	**4.26**	**2.18**	**4.73**	**4.49**
Ventral PPC	L	7/39	4.31	9	−36	−67	44	2.51	**32.77**	**15.25**	**9.72**	**7.42**	1.08	*−3.31*	*−7.02*	*−7.32*	1.76	**3.18**	1.04	**3.91**
Dorsal PPC	L	40	3.88	31	−39	−49	47	1.70	**13.25**	**19.72**	**15.98**	*−4.69*	**13.29**	*−4.01*	**2.88**	*−6.14*	1.44	**7.21**	1.05	**3.93**
Parahip. crtx.	L	35	4.43	6	−21	−34	−13	**5.24**	1.94	**17.94**	*−2.50*	**6.78**	*−2.83*	*−4.23*	*−4.72*	**2.12**	1.02	**2.72**	1.19	**4.49**
Caudate	L	–	4.48	6	−9	8	10	2.08	**10.09**	**21.68**	*−4.48*	1.43	*−3.88*	*−3.55*	*−3.56*	*−1.43*	1.74	**3.40**	1.05	**4.16**
Visual crtx.	L	18	4.47	25	−12	−73	−4	**7.67**	**14.26**	**19.07**	*−3.36*	*−8.04*	0.30	*−0.97*	0.09	**15.16**	**4.84**	**7.01**	0.94	**4.24**

Table shows regions that demonstrated an interaction between memory performance (hit/miss) and memory stage (encoding/retrieval). Outer-left column shows task-based analysis: BA = Brodmann's area; *t* value of task-based effects; Size = cluster size in voxels; coordinates *x*, *y*, and *z* in MNI space. Middle-left column shows *F* values for the 2 × 2 post hoc ANOVA for each cluster: P = memory performance (selected for by task-based analysis), S = memory stage, P × S = interaction. Significant *F* values are indicated in **bold**. Middle-right column shows resting-state effects. Significant *t* values are indicated in **bold**; negative values are listed in italics. Outer-right column shows post hoc tests in the same regions for individual contrasts. Significant *t* values are indicated in **bold**. From left to right: (1) baseline (BASE)–encoding (ENC) hits (HIT), (2) retrieval (RET) hits–baseline, (3) encoding hits–encoding misses (MISS), and (4) retrieval hits–retrieval misses. crtx. = cortex; parahip. = parahippocampal.

To clarify the location of task-induced activity in relation to the intrinsic cortical networks, we conducted the following analysis. First, we isolated the voxels as identified by group-level SPM analysis. Next, for a given cluster of voxels, we computed the average connectivity using the individual's mean connectivity *z* maps. Note that, for each individual, the average connectivity of a cluster is based on the average of 12 seed-based maps (six maps for the motor network) and is computed for each of the six cortical resting-state networks (CON, DMN, DAN, MOT, VAN, and VIS). This results in six-cluster averaged connectivity values for each individual participant. Next, we conducted one-sample *t* tests using the cluster-averaged *z* scores to clarify if a given cluster was significantly overlapping one of six cortical networks (Tables 1–3). For illustration, we show the *t* values from these one-sample *t* tests using spider plots (Figures 3–5). Note, each spider plot is scaled such that the center reflects the lowest (negative) value for each region. *t* values denoting the significance of the connectivity of each activity cluster with each intrinsic cortical network are shown in Tables 1–3.

RESULTS

Behavioral Results

During scanning, retrieval of the prescan face–name pairs resulted in an average of 81 ± 2.6 hits and 34 ± 2.5 misses, whereas the novel pairs resulted in 17 ± 1.8 false alarms and 126 ± 2.6 correct rejections. During the postscan session, retrieval of the scan face–name pairs resulted in 63 ± 3.1 hits and 56 ± 3.1 misses, whereas the novel pairs resulted in 17 ± 1.7 false alarms and 132 ± 1.9 correct rejections. Memory performance (old vs. new), as defined by d-prime (d′), was 1.84 ± 0.08 during the scan session and 1.31 ± 0.09 during the postscan session A *t* test between the d′ indicated that memory performance was better inside than outside the scanner ($p < .001$). During the scan session, on average, 13 of 30 re-paired items were correctly rejected, resulting in a d′ of 0.50 ± 0.04. In the postscan session, 19 of 30 re-paired items were correctly rejected, resulting in a d′ of 0.40 ± 0.10. A *t* test between these "re-paired" d′ scores indicated that performance for the re-paired items was not significantly different inside and outside the scanner ($p = .12$). Note that the re-paired items were not included in the fMRI analysis and only constituted 10% of the trials. During the scan session, the average response time for hits was 1669 ± 36 msec; for miss, 1833 ± 44 msec; for false alarms, 1952 ± 60 msec; for correct rejections, 1589 ± 33 msec; for correctly rejected re-paired items, 1884 ± 51 msec; and for missed re-paired items, 1731 ± 41 msec. During the postscan session, the response time for hits was 1702 ± 73 msec; for miss, 1678 ± 91 msec; for false alarms, 1822 ± 163 msec; for correct rejections, 1689 ± 85 msec; for correctly rejected re-paired items, 1987 ± 124 msec; and for missed re-paired

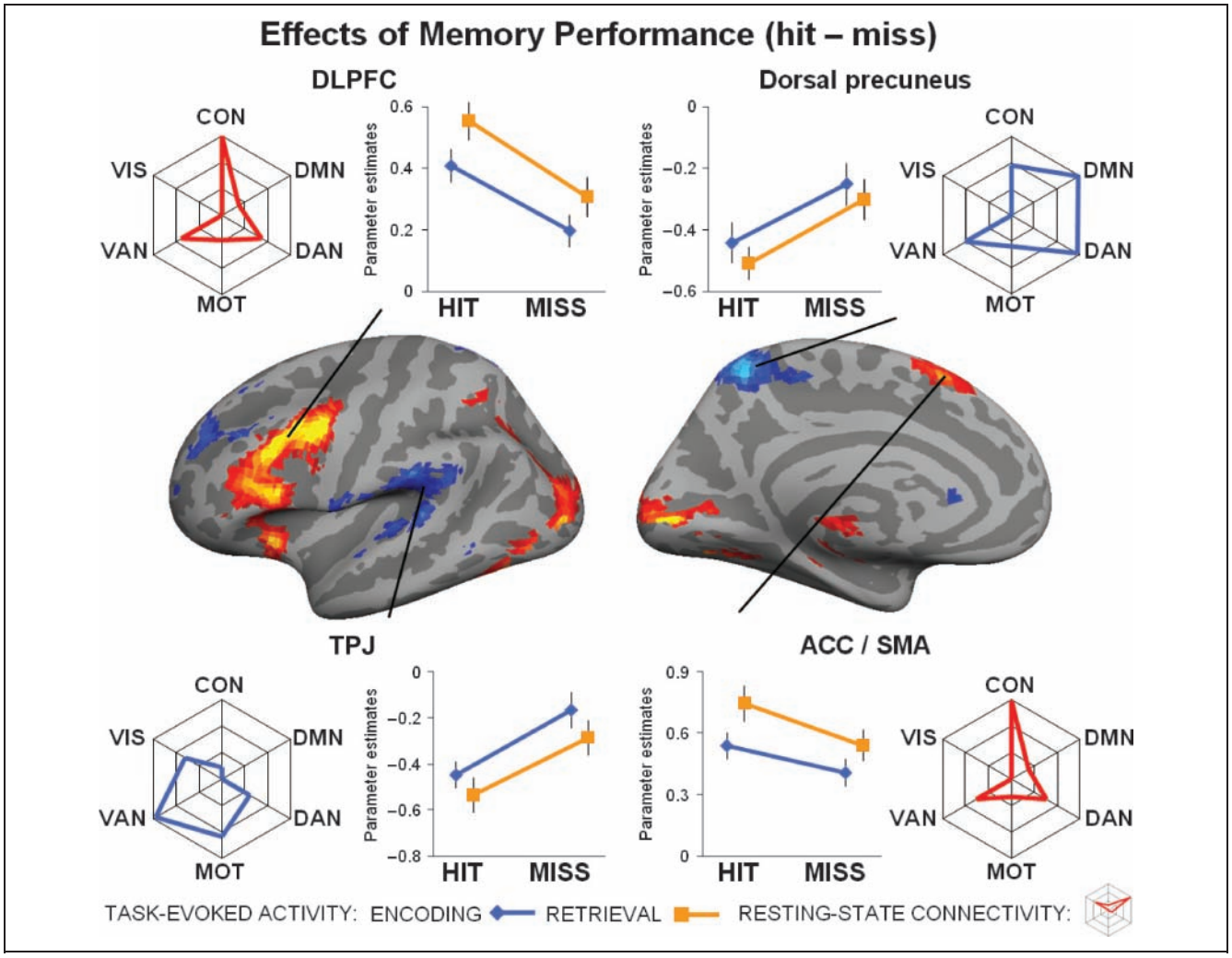

Figure 3. Effects of memory performance: Brain regions on the left hemisphere showing main effect of performance displayed at a threshold of $p < .1$, FDR corrected for visualization purposes only and projected onto the cortical surface. In red, regions showing an effect of successful memory performance (hit > miss). In blue, regions showing an effect of unsuccessful memory performance (miss > hit). Line plots reflect the mean activity for each activated region ($p < .05$, FDR corrected), separately plotted for encoding (blue line) and retrieval (orange line). Spider plots reflect the average connectivity profile for each activated region. Note, each spider plot is scaled such that the center reflects the lowest (often negative) value for each region. The statistical significance for each cluster of activity with each intrinsic cortical network is shown in Table 1. Top left shows activity for the left dorsal precuneus; top right, dorsal precuneus; bottom left, TPJ; and bottom right, ACC/SMA.

items, 2091 ± 139 msec. Paired *t* tests between the scan and postscan response times for hits, miss, false alarms, or correct rejections indicated that the average response times were not significantly different between the scan and postscan sessions.

fMRI Results

We used a 2 × 2 repeated-measures ANOVA of Memory Performance (hit/miss) and Memory Stage (encoding/retrieval) to identify brain regions associated with memory performance, memory stage, and their interaction (the E/R flip; Figure 2A–C). Within the 2 × 2 ANOVA, we directly contrast the factors Performance and Stage. Therefore, activations isolated for unsuccessful performance (misses) are identical to deactivation isolated for successful performance (hits) and likewise for encoding/retrieval activations and deactivations. For simplicity, we present our data in terms of effects of performance, successful memory performance (hit > miss) and unsuccessful memory performance (miss > hits), and memory stage, memory retrieval (retrieval > encoding) and memory encoding (encoding > retrieval). To visualize the intrinsic resting-state networks, we calculated the membership of each voxel with the control, default, dorsal attention, motor, ventral attention, and visual networks using a winner-takes-all approach (Figure 2D), based on the seeds published by Yeo et al. (2011).

Effects of Memory Performance

First, the task-based analysis identified brain regions that showed an effect of memory performance (hit/miss), that

is, regions that showed a significant effect as a function of successful versus unsuccessful memory performance (Figure 3). Several regions, including the dorsolateral PFC (DLPFC) and ACC/supplemental motor area (SMA) showed an effect of successful memory performance (hit > miss; see Table 1 for the full list of regions: $p < .05$, FDR corrected, cluster size > 5). These regions exhibited more activity when memory performance was successful versus unsuccessful. For each significant cluster of activity, we also conducted a second 2 × 2 post hoc ANOVA using the average beta values for encoding hit, encoding miss, retrieval hit, and retrieval miss for each participant to check if these regions demonstrated an effect of Memory Stage (encoding/retrieval) or an interaction between both, in addition to demonstrating effects of memory performance. We found that several regions showing an effect of Performance, including the DLPFC and ACC/SMA, simultaneously showed an effect of Memory Stage, particularly memory retrieval (retrieval > encoding; Table 1). The connectivity analysis indicated that the DLPFC and ACC/SMA were strongly associated with the control network (Table 1). Pair-wise *t* tests confirmed that the left DLPFC and ACC/SMA were more connected to control network than to other significantly connected networks, including ventral and dorsal attention networks (DLPFC: CON > DAN, $p < .001$; CON > VAN, $p < .001$; ACC/SMA: CON > DAN, $p < .001$; CON > VAN, $p < .001$). However, many of the activated brain regions, including the DLPFC and ACC/SMA, showed strong connectivity to multiple networks (Table 1).

The task-based analysis also identified brain regions that showed an effect of successful memory performance

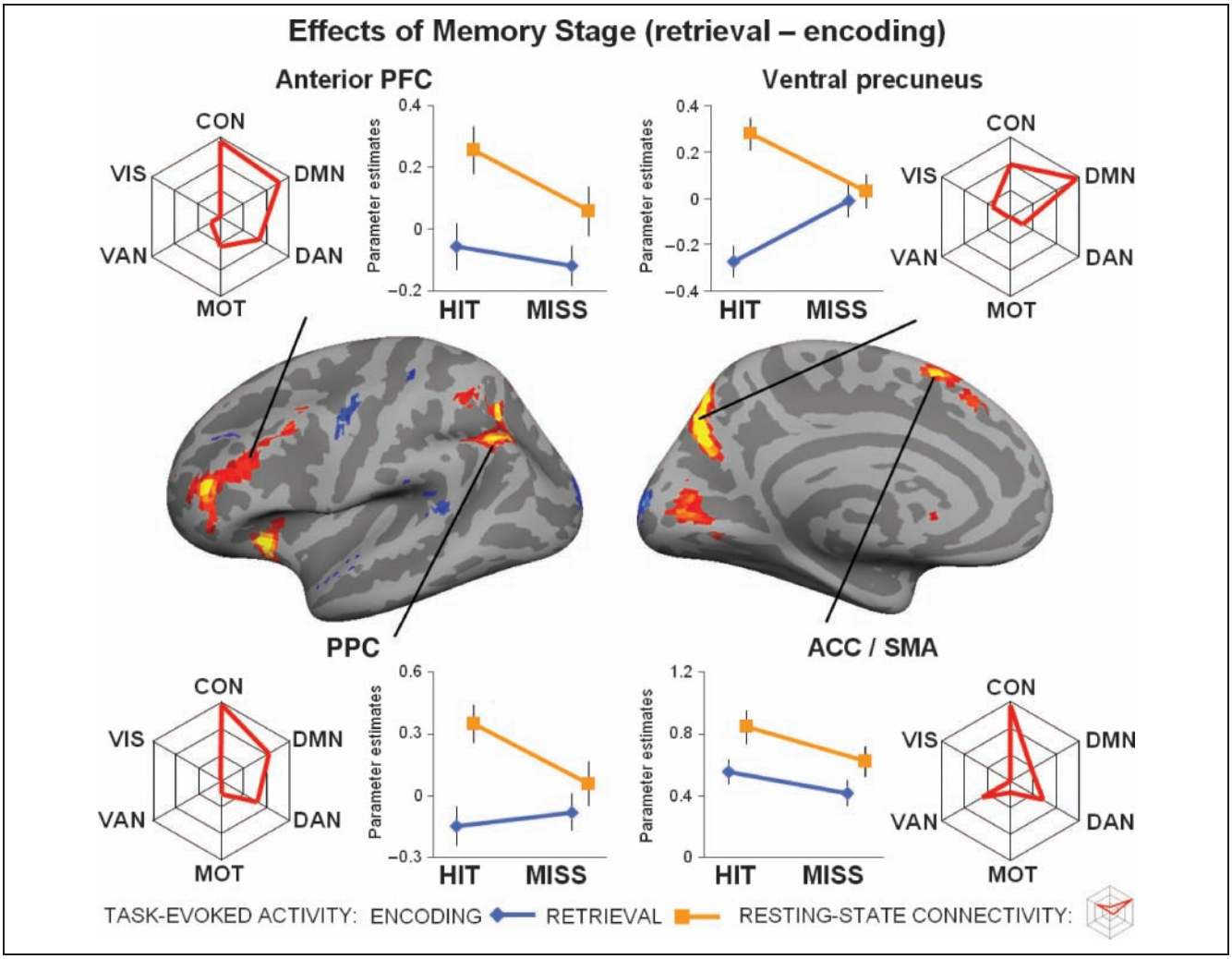

Figure 4. Effects of memory stage: Brain regions on the left hemisphere showing main effect of stage displayed at a threshold of $p < .1$, FDR corrected for visualization purposes only and projected onto the cortical surface. In red, regions showing an effect of memory retrieval (retrieval > encoding). In blue, regions showing an effect of memory encoding (encoding > retrieval). Line plots reflect the mean activity for each activated region ($p < .05$, FDR corrected), separately plotted for encoding (blue line) and retrieval (orange line). Spider plots reflect the average connectivity profile for each activated region. Note, each spider plot is scaled such that the center reflects the lowest (often negative) value for each region. The statistical significance for each cluster of activity with each intrinsic cortical network is shown in Table 2. Top left shows activity for the anterior PFC; top right, ventral precuneus; bottom left, PPC; and bottom right, ACC/SMA.

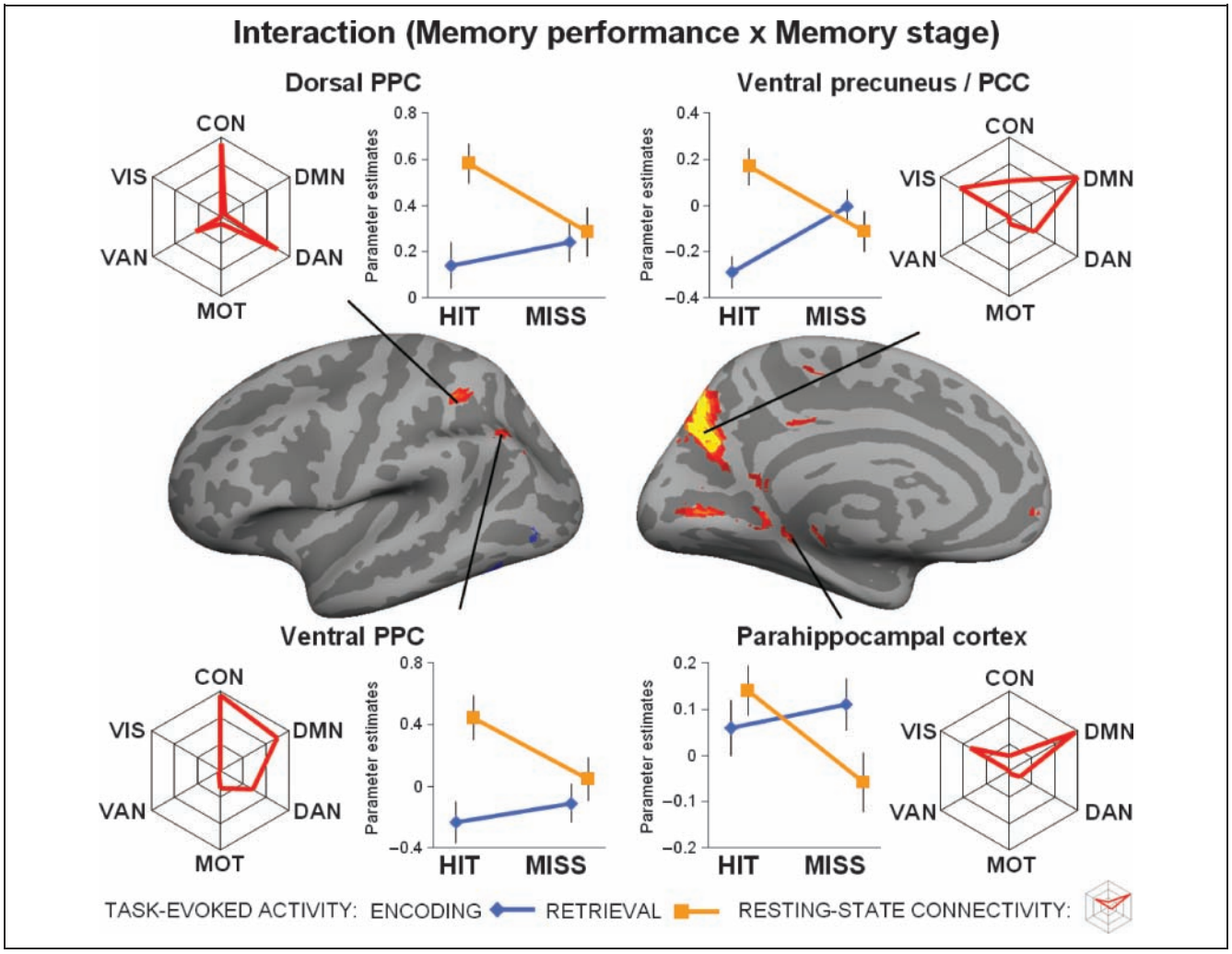

Figure 5. Interaction between performance and stage: Brain regions on the left hemisphere showing an interaction between memory performance (hit/miss) and memory stage (encoding/retrieval) displayed at a threshold of $p < .1$, FDR corrected for visualization purposes only and projected onto the cortical surface. Line plot reflect the mean activity for each activated region ($p < .05$ FDR corrected), separately plotted for encoding (blue line) and retrieval (orange line). Spider plots reflect the average connectivity profile for each activated region. Note, each spider plot is scaled such that the center reflects the lowest (often negative) value for each region. The statistical significance for each cluster of activity with each intrinsic cortical network is shown in Table 3. Top left shows activity for the dorsal PPC; top right, ventral precuneus/PCC; bottom left, ventral PPC; and bottom right, parahippocampal cortex.

(miss > hit). The dorsal precuneus (another subregion of the PMC), bilateral TPJ, and superior PFC (sPFC) displayed more activity during unsuccessful versus successful memory performance (Figure 3; see Table 1 for the full list of regions: $p < .05$, FDR corrected, cluster size > 5). For each significant cluster of activity, we conducted a 2 × 2 post hoc ANOVA to evaluate whether these regions also showed an effect of Memory Stage or an interaction. We found that TPJ showed an effect of Memory Stage, in particular, encoding (encoding > retrieval: Table 1). The connectivity analysis indicated that the dorsal precuneus, TPJ, and sPFC were all associated with the ventral attention network (Table 1). Pair-wise t tests demonstrated that dorsal precuneus was more strongly connected to both the default network and dorsal attention network (dorsal precuneus: VAN < DMN, $p = .0047$; VAN < DAN, $p < .001$), whereas connectivity between the default network and dorsal attention network was not significantly different (DAN < DMN, $p = .87$). Both the left and right TPJ showed the strongest connection to ventral attention network (right TPJ: VAN > DAN, $p < .001$; VAN > CON, $p < .001$); although for the left TPJ, the connectivity difference between motor and ventral attention network was only trending (left TPJ: VAN > VIS, $p < .001$; VAN > MOT, $p = .078$). These results again demonstrate that many of the activated brain regions showed strong connectivity to multiple networks. In general, these findings demonstrate that effect of successful memory performance occurs in regions connected to the control network, whereas the effect of unsuccessful memory performance occurs in regions connected to the ventral attention network.

Effects of Memory Stage

Second, the task-based analysis identified brain regions that showed an effect of Memory Stage (encoding/retrieval); that is, regions that display a significant difference as a function of retrieval versus encoding (Figure 4). The ventral precuneus (a subregion of the PMC), PPC, anterior PFC, and ACC/SMA showed an effect of memory retrieval stage (retrieval > encoding). These regions exhibited more activity when retrieving previously seen information (old) than when encoding novel information (new; see Table 2 for the full list of regions: $p < .05$, FDR corrected, cluster size > 5). For each significant cluster of activity, we conducted a 2 × 2 post hoc ANOVA to evaluate whether these regions also showed an effect of Memory Performance or an interaction. Several regions, including ventral precuneus and PPC, also showed an interaction with Memory Performance (Table 2). Several other regions, including ACC/SMA, showed an effect of successful memory but no interaction, in addition to the effect of memory retrieval. Connectivity analyses indicated that many of these regions, including the ventral precuneus, PPC, anterior PFC, and ACC/SMA were strongly connected to the control network and default network. Pair-wise *t* tests demonstrated that the PPC and ACC/SMA showed the greatest connectivity to the control network (left PPC: CON > DMN, $p = .013$; CON > DAN, $p < .001$; right PPC: CON > DMN, $p < .001$; CON > DAN, $p < .001$; ACC/SMA: CON > DAN, $p < .001$; CON > VAN, $p < .001$). In contrast, the left ventral precuneus was predominantly connected to the default network (DMN > CON, $p < .001$).

The task-based analysis also identified brain regions that showed an effect of memory encoding stage (encoding > retrieval; Figure 4). The visual cortex and left anterior displayed more activity during memory encoding versus retrieval (Figure 2; see Table 2 for the full list of regions: $p < .05$, FDR corrected, cluster size > 5). For each significant cluster of activity, we conducted a 2 × 2 post hoc ANOVA to evaluate whether regions also showed an effect of Memory Performance or an interaction (Table 2). The anterior PFC also showed an effect of unsuccessful memory performance. Next, the connectivity analysis of the activated clusters indicated that the anterior PFC showed strong connectivity to both dorsal and ventral attention networks. Pair-wise *t* tests demonstrated that the anterior PFC was predominantly connected to the ventral attention network (anterior PFC: VAN > DAN, $p < .001$; VAN > CON, $p < .001$), whereas the region in the visual cortex was predominantly connected to the visual network (Table 2). In general, these findings indicate that a number of brain regions activated by memory retrieval are connected to both the control network and default network.

Interactions between Memory Performance and Memory Stage

Finally, the task-based analysis also identified brain regions that showed an interaction between memory performance and memory stage (Figure 5, Table 3), including the ventral precuneus/posterior cingulate cortex (PCC, another subregion of the PMC), left dorsal and ventral PPC, and parahippocampal cortex. Note that, for each cluster of activity, we tested the direction of interaction. All clusters demonstrated more activity during encoding and less activity during retrieval. No cluster of activity that survived the threshold ($p < .05$, FDR corrected) demonstrated the reverse interaction. For each significant cluster of activity, we conducted a 2 × 2 post hoc ANOVA to evaluate whether the regions also showed a main effect of Memory Performance or Memory Stage. In addition to the interaction, the ventral precuneus/PCC and the dorsal and ventral PPC showed an effect of memory retrieval, whereas the parahippocampal cortex at the same time showed an effect of successful memory performance. Note that these effects are included for completeness and should be interpreted cautiously because of the interaction. To identify if the location of the interaction overlapped with the original definition of the E/R flip (Daselaar et al., 2009), we conducted a control analysis defining the E/R flip as the conjunction between encoding miss–encoding hit ($p < .05$, FDR corrected) and retrieval hit–retrieval miss ($p < .05$, FDR corrected). Two cluster in the ventral precuneus survived this strict conjunctive threshold: (left precuneus: cluster size = 37, *t* max [encoding] = 5.16, MNI [*x*,*y*,*z*; encoding] = −16, −70,26, *t* max [retrieval] = 4.63, MNI [*x*,*y*,*z*; retrieval] = −13,−70,29; right precuneus: cluster size = 3, *t* max [encoding] = 3.91, MNI [*x*,*y*,*z*; encoding] = 14,−73,29, *t* max [retrieval] = 3.99, MNI [*x*,*y*,*z*; retrieval] = 14, −73,29). Furthermore, the maxima as identified by interaction (MNI [*x*,*y*,*z*] = 12,−70,26) overlapped with the conjunction analysis, indicating that the interaction within the ventral precuneus/PCC was driven by the E/R flip (see also post hoc tests in Table 3).

Next, the connectivity analysis indicated that many of these brain regions, including the ventral precuneus/PCC, ventral PPC, and parahippocampal cortex, showed strong connectivity to the default network (Table 3). Pair-wise *t* tests demonstrated that connectivity of the ventral precuneus was stronger to the default network than control network (DMN > CON, $p = .009$) but not significantly different between visual and default network (DMN > VIS, $p = .13$). The ventral PPC demonstrated connectivity to both control and default network, and also, this connectivity was not significantly different (DMN > CON, $p = .70$). The parahippocampal cortex was predominantly connected to the default network (DMN > VIS, $p = .0014$). The dorsal PPC was not significantly connected to the default network but, instead, was similarly connected to the control network and dorsal attention network (CON > DAN, $p = .88$). Similar to the effects of performance and stage, almost all of the activated clusters demonstrating an interaction were connected to multiple cortical networks. Below, we discuss these neuroimaging results in relation to the E/R flip.

DISCUSSION

In this event-related fMRI study, we identified activity patterns related to memory performance (hit/miss), memory stage (encoding/retrieval), and their interaction. Using resting-state functional connectivity analysis, we examined the intrinsic networks associated with regions showing each activity pattern. First, we found an effect of successful memory performance in brain regions connected to the control network and an effect of unsuccessful memory performance in regions connected to the ventral attention network. Second, we found an effect of memory retrieval in regions spanning both control and default networks. Third, we found an interaction between memory performance and memory stage in regions associated with the default network, a pattern related to the E/R flip.

Effects of Memory Performance

A set of regions, most notably the DLPFC, demonstrated an effect of successful memory performance (Figure 3). These findings are coherent with neuroimaging studies that link these regions to cognitive control (Niendam et al., 2012). The left DLPFC also showed a significant effect of memory retrieval, which corresponds to a recent meta-analysis comparing encoding and retrieval (Spaniol et al., 2009). The overlap in the DLPFC between both effects of successful memory performance and memory retrieval is consistent with a critical role in episodic memory. Clinical studies indicate that cortical damage or TMS to the DLPFC can result in memory impairments (Alexander, Stuss, & Fansabedian, 2003; Rossi et al., 2001). The connectivity analysis indicates that the left DLPFC was predominantly connected to the control network. However, the DLPFC also showed strong connectivity to both the ventral and dorsal attention networks. Thus, the DLPFC appears to be functionally connected to multiple cortical networks and, as such, may integrate information across the dorsal, ventral, and control networks.

A second set of regions, most notably the dorsal precuneus and TPJ, demonstrated an effect of unsuccessful memory performance (Figure 3). These findings are consistent with neuroimaging studies linking task-induced deactivations to successful cognitive performance (Huijbers, Pennartz, Rubin, & Daselaar, 2011; McKiernan, Kaufman, Kucera-Thompson, & Binder, 2003; Mazoyer et al., 2001). The TPJ also showed a significant effect of memory encoding, again in line with a recent meta-analysis (Spaniol et al., 2009). The overlap between both effects of unsuccessful memory performance and memory encoding within the TPJ also suggests that this region plays an important role in episodic memory. However, it remains unclear if the effect of performance should be interpreted in terms of beneficial deactivations or detrimental activations (Daselaar et al., 2004; Otten & Rugg, 2001). In line with the latter "detrimental" interpretation, TPJ activity is sometimes interpreted in terms of bottom–up distractions (Corbetta, Patel, & Shulman, 2008; Weissman et al., 2006). The connectivity analysis indicated that the TPJ was strongly connected to the ventral attention network, suggestive of a bottom–up function. In contrast, the dorsal precuneus also showed an effect unsuccessful memory performance but, unlike the TPJ, did not show an effect of memory stage. The connectivity analysis also indicated that the dorsal precuneus was more connected to the default and dorsal attention networks. Together, these findings are consistent with recent studies that found encoding-related deactivations in both the TPJ and the default network (Anticevic et al., 2010) and support the idea that effects of performance are not restricted to regions within the default network (Spreng, 2012).

Effects of Memory Stage

A third set of brain regions, most notably the ventral precuneus and PPC, demonstrated an effect of memory retrieval (Figure 4), displaying more activity during retrieval compared with encoding. These findings converge with fMRI studies comparing previously seen (old) with novel (new) information (Hayama, Vilberg, & Rugg, 2012; Spaniol et al., 2009; Wagner, Shannon, Kahn, & Buckner, 2005). We also found some regions that displayed more activity during encoding compared with retrieval, an effect of memory encoding, (Figure 4, Table 2). The connectivity analysis indicated that many of the regions showing an effect of retrieval were connected to the control and default networks. Note that, although we used a face–name paradigm, the task included few re-paired items, making it essentially a recognition paradigm. Memory performance—as defined by d-prime (d′)—was very high for distinguishing old versus new pairs but relatively poor for discriminating re-paired items (see Results). Accordingly, in the fMRI analysis, we excluded re-paired items. Thus, the effects of memory stage are likely to reflect neurocorrelates related to recognition memory (familiarity) rather then associative memory retrieval (recollection). This interpretation is supported by the fMRI results, because the effect of retrieval seems to occur in brain regions commonly linked to familiarity (Vilberg & Rugg, 2007). Similar coactivations in regions spanning the control and default networks have recently been reported in studies of autobiographical memory retrieval (Gerlach, Spreng, Gilmore, & Schacter, 2011; Spreng et al., 2010). Of importance, we demonstrate that several regions in the default network, including the ventral precuneus and PPC, demonstrate not only an effect of memory retrieval but also an interaction between memory performance and memory stage. This finding indicates that activity in parietal regions is likely to reflect distinct cognitive processes operating during the encoding and retrieval stages. The interaction demonstrates that

the effects of memory stage in the ventral precuneus and PPC cannot be interpreted in terms of encoding/retrieval alone.

Interactions between Performance and Stage

Several regions demonstrated an interaction between memory performance and memory stage, including the ventral precuneus/PCC, the dorsal and ventral PPC, and the parahippocampal cortex (Figure 5). Most previous memory studies tested encoding and retrieval stages in separate experimental sessions (see, however, Gilbert et al., 2011) and modeled the effects of both memory stages separately. The current design measured encoding and retrieval simultaneously, and this allows simultaneous modeling of effects of performance (hit/miss) and stage (encoding/retrieval). As a consequence, the E/R flip—as defined by the interaction—cannot be explained by shifts in the fMRI baseline (Gusnard & Raichle, 2001; Stark & Squire, 2001). Note that previous E/R-flip studies vary in terms of the contrasts used to define the E/R flip, either using hits versus misses (Daselaar et al., 2009) or contrasting hits versus fixation (Vannini et al., 2011). Results between these studies also vary in terms of locating an E/R flip in the PPC or medial PFC. Yet, across studies, the E/R flip was consistently reported in the ventral precuneus/PCC (Huijbers et al., 2012). The control analysis (see Results) also demonstrated that only ventral precuneus/PCC shows an E/R flip when defined by a whole-brain conjunction (Daselaar et al., 2009). Post hoc *t* tests further confirmed that the ventral precuneus/PCC—as identified by the interaction—demonstrated an E/R flip regardless of the exact contrast definition (Table 3). The connectivity analysis indicated that the ventral precuneus/PCC and ventral PPC were connected to the default network, confirming previous studies that combined task and resting-state fMRI data (Huijbers, Pennartz, Cabeza, et al., 2011). Together, these findings provide strong support for the hypothesis that the E/R flip represents an interaction between performance-related deactivations during encoding and activations during retrieval that both occur within the posteromedial and possibly other default-mode regions.

In addition to the interaction, the ventral precuneus/PCC and ventral PPC also showed an effect of memory retrieval. These findings may have consequences for understanding the contribution of the parietal cortices to episodic memory. Typical activation patterns observed in the parietal cortices—when contrasting previously seen (old) and novel (new) information—should be interpreted in terms of successful and unsuccessful encoding and retrieval processes. One recent hypothesis suggests that the E/R flip in the ventral PPC can be explained in terms of reorienting by bottom–up attention to memory (AtoM; Cabeza, Ciaramelli, Olson, & Moscovitch, 2008; Ciaramelli, Grady, & Moscovitch, 2008). The bottom–up attention, as described by AtoM, hypothesizes that, during encoding, external to-be-encoded information that is typically in the focus of attention and reorienting is likely to coincide with distraction by unrelated stimuli or internal thoughts (Cabeza, Ciaramelli, & Moscovitch, 2012). Yet, during retrieval, successful performance requires that attention is reoriented from external cues guiding the task toward internal information retrieved from episodic memory. The E/R flip may therefore reflect the interaction between activation driven by external sources that are beneficial during encoding but detrimental during retrieval. This would account for our observed interaction between memory performance and memory stage. However, our findings also indicate that the TPJ, the region most commonly linked to bottom–up attention (Corbetta et al., 2008), showed an effect of unsuccessful memory performance during both memory stages and did not exhibit an interaction. Thus, our findings dissociate the TPJ from the dorsal and ventral PPC consistent with a review of encoding processes in the parietal cortices (Uncapher & Wagner, 2009). However, the current results also demonstrate how subtle this dissociation may be, because the TPJ and ventral PCC show a distinct pattern during retrieval but a similar pattern during encoding. Whether the AtoM account can be extended to the medial parietal cortices (ventral precuneus/PCC) or if another cognitive process such as self-referential processes can explain the E/R flip in the ventral precuneus/PCC remains a topic of current debate (Huijbers et al., 2012).

We also found an interaction in the parahippocampal cortex, a finding not previously reported (e.g., Daselaar et al., 2009). The hippocampus. in contrast to the parahippocampus, is known to show patterns of activity distinct from the E/R flip, as it is commonly not deactivated during memory encoding (Huijbers, Pennartz, Cabeza, et al., 2011; Vannini et al., 2011). Although functional connectivity studies have demonstrated connectivity between the medial-temporal lobe and the default network (Kahn, Andrews-Hanna, Vincent, Snyder, & Buckner, 2008; Greicius, Krasnow, Reiss, & Menon, 2003), recent results indicate that this connectivity is mediated via the parahippocampal cortex (Ward et al., in press; Libby, Ekstrom, Ragland, & Ranganath, 2012). In line with this possibility, the connectivity analysis confirmed that the location of the interaction effect within the parahippocampus was predominantly connected to the default network (Figure 5). The interaction with the parahippocampus is also consistent with the hypothesis that the hippocampus is coupled with the default network during memory retrieval but not during memory encoding (Huijbers, Pennartz, Cabeza, et al., 2011). The parahippocampus also showed connectivity with the visual network. These data suggest that the parahippocampus could mediate the effective connectivity between the hippocampus and the visual or default network during encoding and retrieval. For example, the parahippocampus could gate hippocampal activity so that it is associated with the visual cortex during memory encoding but with the default network during retrieval. Future studies

should explore the dynamics of parahippocampal connectivity, because a loss of medial-temporal lobe connectivity is believed to underlie memory problems associated with Alzheimer's disease (Hedden et al., 2009; Allen et al., 2007; Wang et al., 2006; Greicius, Srivastava, Reiss, & Menon, 2004). In summary, the interaction demonstrates that, within several brain regions including the PMC and PPC, a simple contrast between old versus new items should be interpreted with caution, as activity is dependent on both memory stage and memory performance.

Task-induced Activity versus Resting-state Functional Connectivity

In general, our findings indicate that task-induced activity is not restricted within the boundaries of intrinsic cortical networks as identified by resting-state functional connectivity. Rather, task-induced activity often occurs in brain regions spanning multiple cortical networks (Tables 1–3). Other recent task-based fMRI studies have also reported task-based activity outside the boundaries of a single cortical network (Anticevic et al., 2010; Spreng et al., 2010). This mismatch between task-based activity and functional connectivity might be fundamental to the underlying neuronal processes. Resting-state functional connectivity is primarily driven by slow periodic fluctuations in the BOLD signal (Biswal et al., 1995). Moreover, these fluctuations likely reflect an indirect measure for anatomical connectivity, as they are restrained by the anatomy of the brain (Van Dijk et al., 2010; Fox & Raichle, 2007). Task-evoked changes in BOLD signal are believed to reflect the brain's metabolic response to the activity of populations of neurons and correlate with local field potentials (Logothetis, Pauls, Augath, Trinath, & Oeltermann, 2001; Ogawa, Lee, Kay, & Tank, 1990). Thus, the mismatch between task-based activity and resting-state functional connectivity might simply reflect task-induced BOLD activity versus coherent slow periodic changes in BOLD signal that occur throughout large networks. However, this does not imply that cognitive processes do not alter the connectivity of large-scale intrinsic cortical networks. The connectivity of cortical networks can be detected within task-based fMRI data and may be modulated by cognitive processes (Niazy, Xie, Miller, Beckmann, & Smith, 2011; Andrews-Hanna, Reidler, Huang, et al., 2010; Albert, Robertson, Mehta, & Miall, 2009). Yet, if we assume that functional connectivity primarily reflects the underlying anatomy of the brain, our findings may simply imply that task-induced effects are likely to occur in regions situated in-between or associated with multiple large-scale networks.

Conclusion

In this study, we identified the neural correlates of memory performance (hit/miss) and memory stage (encoding/retrieval), the interaction between these processes, and the relationship to large-scale intrinsic networks identified during the resting state. First, we found an effect of successful memory performance in brain regions associated with the control network and an effect of unsuccessful memory performance in brain regions associated with the ventral attention network. Second, we found an effect of memory retrieval in brain regions that tend to span the default network and control network. Third, we found an interaction between memory performance and memory stage in regions associated with the default network. Together, these findings demonstrate that the task-based effects of memory performance and memory stage dissociate regions connected to the default network and occur in regions that span multiple networks.

Acknowledgments

This work was supported by the European Molecular Biology Organization: ALTF 318-2011 (W. H.), the Marie Curie Fellowship: FP7-PEOPLE-2007-4-1-IOF from the European Union (P. V.), the Swedish Brain Foundation and Swedish Society for Medicine (P. V.), the National Institutes of Health: K01 AG040197 (T. H.), K24 AG035007 (R. S.), R01 AG027435-S1 (R. S.), P01AG036694 (R. S.), P50AG00513421 (R. S.), and the Alzheimer's Association: IIRG-06-27374 (R. S.). This research was carried out in part at the Athinoula A. Martinos Center for Biomedical Imaging at the Massachusetts General Hospital, using resources provided by the Center for Functional Neuroimaging Technologies, P41EB015896, a P41 Regional Resource supported by the National Institute of Biomedical Imaging and Bioengineering (NIBIB), National Institutes of Health. The content is solely the responsibility of the authors and does not necessarily represent the official view of the NIH.

Reprint requests should be sent to Willem Huijbers, Athinoula A. Martinos Center for Biomedical Imaging, 149 Thirteenth Street, Suite 2301, Charlestown, Massachusetts 02129 or via e-mail: huijbers@nmr.mgh.harvard.edu.

REFERENCES

Albert, N. B., Robertson, E. M., Mehta, P., & Miall, R. C. (2009). Resting state networks and memory consolidation. *Communicative & Integrative Biology, 2,* 530–532.

Alexander, M. P., Stuss, D. T., & Fansabedian, N. (2003). California Verbal Learning Test: Performance by patients with focal frontal and non-frontal lesions. *Brain, 126,* 1493–1503.

Allen, G., Barnard, H., McColl, R., Hester, A. L., Fields, J. A., Weiner, M. F., et al. (2007). Reduced hippocampal functional connectivity in Alzheimer disease. *Archives of Neurology, 64,* 1482–1487.

Andrews-Hanna, J. R., Reidler, J. S., Huang, C., & Buckner, R. L. (2010). Evidence for the default network's role in spontaneous cognition. *Journal of Neurophysiology, 104,* 322–335.

Andrews-Hanna, J. R., Reidler, J. S., Sepulcre, J., Poulin, R., & Buckner, R. L. (2010). Functional–anatomic fractionation of the brain's default network. *Neuron, 65,* 550–562.

Anticevic, A., Repovs, G., Shulman, G. L., & Barch, D. M. (2010). When less is more: TPJ and default network deactivation during encoding predicts working memory performance. *Neuroimage, 49,* 2638–2648.

Biswal, B., Yetkin, F. Z., Haughton, V. M., & Hyde, J. S. (1995). Functional connectivity in the motor cortex of resting human

brain using echo-planar MRI. *Magnetic Resonance in Medicine, 34,* 537–541.
Brainard, D. H. (1997). The psychophysics toolbox. *Spatial Vision, 10,* 433–436.
Cabeza, R., Ciaramelli, E., & Moscovitch, M. (2012). Cognitive contributions of the ventral parietal cortex: An integrative theoretical account. *Trends in Cognitive Sciences, 16,* 338–352.
Cabeza, R., Ciaramelli, E., Olson, I. R., & Moscovitch, M. (2008). The parietal cortex and episodic memory: An attentional account. *Nature Reviews Neuroscience, 9,* 613–625.
Ciaramelli, E., Grady, C. L., & Moscovitch, M. (2008). Top–down and bottom–up attention to memory: A hypothesis (AtoM) on the role of the posterior parietal cortex in memory retrieval. *Neuropsychologia, 46,* 1828–1851.
Corbetta, M., Patel, G., & Shulman, G. L. (2008). The reorienting system of the human brain: From environment to theory of mind. *Neuron, 58,* 306–324.
Dale, A. M., Greve, D. N., & Burock, M. A. (1999, June 11–16). *Optimal stimulus sequences for event-related fMRI*. Paper presented at the 5th International Conference on Functional Mapping of the Human Brain, Duesseldorf, Germany.
Damoiseaux, J. S., Prater, K. E., Miller, B. L., & Greicius, M. D. (2012). Functional connectivity tracks clinical deterioration in Alzheimer's disease. *Neurobiology of Aging, 33,* 828.
Daselaar, S. M., Prince, S. E., & Cabeza, R. (2004). When less means more: Deactivations during encoding that predict subsequent memory. *Neuroimage, 23,* 921–927.
Daselaar, S. M., Prince, S. E., Dennis, N. A., Hayes, S. M., Kim, H., & Cabeza, R. (2009). Posterior midline and ventral parietal activity is associated with retrieval success and encoding failure. *Frontiers in Human Neuroscience, 3,* 13.
Fischl, B., Rajendran, N., Busa, E., Augustinack, J., Hinds, O., Yeo, B. T., et al. (2008). Cortical folding patterns and predicting cytoarchitecture. *Cerebral Cortex, 18,* 1973–1980.
Fox, M. D., & Raichle, M. E. (2007). Spontaneous fluctuations in brain activity observed with functional magnetic resonance imaging. *Nature Reviews Neuroscience, 8,* 700–711.
Gerlach, K. D., Spreng, R. N., Gilmore, A. W., & Schacter, D. L. (2011). Solving future problems: Default network and executive activity associated with goal-directed mental simulations. *Neuroimage, 55,* 1816–1824.
Gilbert, S. J., Armbruster, D. J. N., & Panagiotidi, M. (2011). Similarity between brain activity at encoding and retrieval predicts successful realization of delayed intentions. *Journal of Cognitive Neuroscience, 24,* 1–13.
Greicius, M. D., Krasnow, B., Reiss, A. L., & Menon, V. (2003). Functional connectivity in the resting brain: A network analysis of the default mode hypothesis. *Proceedings of the National Academy of Sciences, U.S.A., 100,* 253–258.
Greicius, M. D., Srivastava, G., Reiss, A. L., & Menon, V. (2004). Default-mode network activity distinguishes Alzheimer's disease from healthy aging: Evidence from functional MRI. *Proceedings of the National Academy of Sciences, U.S.A., 101,* 4637–4642.
Gusnard, D. A., & Raichle, M. E. (2001). Searching for a baseline: Functional imaging and the resting human brain. *Nature Reviews Neuroscience, 2,* 685–694.
Hayama, H. R., Vilberg, K. L., & Rugg, M. D. (2012). Overlap between the neural correlates of cued recall and source memory: Evidence for a generic recollection network? *Journal of Cognitive Neuroscience, 24,* 1127–1137.
Hayden, B. Y., Smith, D. V., & Platt, M. L. (2009). Electrophysiological correlates of default-mode processing in macaque posterior cingulate cortex. *Proceedings of the National Academy of Sciences, U.S.A., 106,* 5948–5953.
Hedden, T., Van Dijk, K. R., Becker, J. A., Mehta, A., Sperling, R. A., Johnson, K. A., et al. (2009). Disruption of functional connectivity in clinically normal older adults harboring amyloid burden. *Journal of Neuroscience, 29,* 12686–12694.
Huijbers, W., Pennartz, C. M., Cabeza, R., & Daselaar, S. M. (2009). When learning and remembering compete: A functional MRI study. *PLoS Biology, 7,* e11.
Huijbers, W., Pennartz, C. M., Cabeza, R., & Daselaar, S. M. (2011). The hippocampus is coupled with the default network during memory retrieval but not during memory encoding. *PLoS One, 6,* e17463.
Huijbers, W., Pennartz, C. M., Rubin, D. C., & Daselaar, S. M. (2011). Imagery and retrieval of auditory and visual information: Neural correlates of successful and unsuccessful performance. *Neuropsychologia, 49,* 1730–1740.
Huijbers, W., Vannini, P., Sperling, R. A., C. M. P., Cabeza, R., & Daselaar, S. M. (2012). Explaining the encoding/retrieval flip: Memory-related deactivations and activations in the posteromedial cortex. *Neuropsychologia, 50,* 3764–3774.
Hutchinson, J. B., Uncapher, M. R., & Wagner, A. D. (2009). Posterior parietal cortex and episodic retrieval: Convergent and divergent effects of attention and memory. *Learning and Memory, 16,* 343–356.
Kahn, I., Andrews-Hanna, J. R., Vincent, J. L., Snyder, A. Z., & Buckner, R. L. (2008). Distinct cortical anatomy linked to subregions of the medial temporal lobe revealed by intrinsic functional connectivity. *Journal of Neurophysiology, 100,* 129–139.
Kim, H. (2011). Neural activity that predicts subsequent memory and forgetting: A meta-analysis of 74 fMRI studies. *Neuroimage, 54,* 2446–2461.
Kim, H., Daselaar, S. M., & Cabeza, R. (2010). Overlapping brain activity between episodic memory encoding and retrieval: Roles of the task-positive and task-negative networks. *Neuroimage, 49,* 1045–1054.
Konishi, S., Wheeler, M. E., Donaldson, D. I., & Buckner, R. L. (2000). Neural correlates of episodic retrieval success. *Neuroimage, 12,* 276–286.
Leech, R., Kamourieh, S., Beckmann, C. F., & Sharp, D. J. (2011). Fractionating the default mode network: Distinct contributions of the ventral and dorsal posterior cingulate cortex to cognitive control. *Journal of Neuroscience, 31,* 3217–3224.
Libby, L. A., Ekstrom, A. D., Ragland, J. D., & Ranganath, C. (2012). Differential connectivity of perirhinal and parahippocampal cortices within human hippocampal subregions revealed by high-resolution functional imaging. *Journal of Neuroscience, 32,* 6550–6560.
Logothetis, N. K., Pauls, J., Augath, M., Trinath, T., & Oeltermann, A. (2001). Neurophysiological investigation of the basis of the fMRI signal. *Nature, 412,* 150–157.
Mazoyer, B., Zago, L., Mellet, E., Bricogne, S., Etard, O., Houde, O., et al. (2001). Cortical networks for working memory and executive functions sustain the conscious resting state in man. *Brain Research Bulletin, 54,* 287–298.
McKiernan, K. A., Kaufman, J. N., Kucera-Thompson, J., & Binder, J. R. (2003). A parametric manipulation of factors affecting task-induced deactivation in functional neuroimaging. *Journal of Cognitive Neuroscience, 15,* 394–408.
Minear, M., & Park, D. C. (2004). A lifespan database of adult facial stimuli. *Behavior Research Methods, Instruments, & Computers, 36,* 630–633.
Niazy, R. K., Xie, J., Miller, K., Beckmann, C. F., & Smith, S. M. (2011). Spectral characteristics of resting state networks. *Progress in Brain Research, 193,* 259–276.

Niendam, T., Laird, A., Ray, K., Dean, Y., Glahn, D., & Carter, C. (2012). Meta-analytic evidence for a superordinate cognitive control network subserving diverse executive functions. *Cognitive, Affective, & Behavioral Neuroscience, 12,* 241–268.

Ogawa, S., Lee, T. M., Kay, A. R., & Tank, D. W. (1990). Brain magnetic resonance imaging with contrast dependent on blood oxygenation. *Proceedings of the National Academy of Sciences, U.S.A. 87,* 9868–9872.

Otten, L. J., & Rugg, M. D. (2001). When more means less: Neural activity related to unsuccessful memory encoding. *Current Biology, 11,* 1528–1530.

Rossi, S., Cappa, S. F., Babiloni, C., Pasqualetti, P., Miniussi, C., Carducci, F., et al. (2001). Prefrontal [correction of Prefontal] cortex in long-term memory: An "interference" approach using magnetic stimulation. *Nature Neuroscience, 4,* 948–952.

Schacter, D. L., Buckner, R. L., Koutstaal, W., Dale, A. M., & Rosen, B. R. (1997). Late onset of anterior prefrontal activity during true and false recognition: An event-related fMRI study. *Neuroimage, 6,* 259–269.

Seeley, W. W., Menon, V., Schatzberg, A. F., Keller, J., Glover, G. H., Kenna, H., et al. (2007). Dissociable intrinsic connectivity networks for salience processing and executive control. *Journal of Neuroscience, 27,* 2349–2356.

Shrager, Y., Kirwan, C. B., & Squire, L. R. (2008). Activity in both hippocampus and perirhinal cortex predicts the memory strength of subsequently remembered information. *Neuron, 59,* 547–553.

Smith, S. M., Fox, P. T., Miller, K. L., Glahn, D. C., Fox, P. M., Mackay, C. E., et al. (2009). Correspondence of the brain's functional architecture during activation and rest. *Proceedings of the National Academy of Sciences, U.S.A., 106,* 13040–13045.

Spaniol, J., Davidson, P. S., Kim, A. S., Han, H., Moscovitch, M., & Grady, C. L. (2009). Event-related fMRI studies of episodic encoding and retrieval: Meta-analyses using activation likelihood estimation. *Neuropsychologia, 47,* 1765–1779.

Sperling, R. A., Bates, J. F., Chua, E. F., Cocchiarella, A. J., Rentz, D. M., Rosen, B. R., et al. (2003). fMRI studies of associative encoding in young and elderly controls and mild Alzheimer's disease. *Journal of Neurology, Neurosurgery and Psychiatry, 74,* 44–50.

Sperling, R. A., Bates, J. F., Cocchiarella, A. J., Schacter, D. L., Rosen, B. R., & Albert, M. S. (2001). Encoding novel face–name associations: A functional MRI study. *Human Brain Mapping, 14,* 129–139.

Spreng, R. N. (2012). The fallacy of a "task-negative" network. *Frontiers in Psychology, 3,* 145.

Spreng, R. N., Stevens, W. D., Chamberlain, J. P., Gilmore, A. W., & Schacter, D. L. (2010). Default network activity, coupled with the frontoparietal control network, supports goal-directed cognition. *Neuroimage, 53,* 303–317.

Stark, C. E., & Squire, L. R. (2001). When zero is not zero: The problem of ambiguous baseline conditions in fMRI. *Proceedings of the National Academy of Sciences, U.S.A., 98,* 12760–12766.

Uncapher, M. R., & Wagner, A. D. (2009). Posterior parietal cortex and episodic encoding: Insights from fMRI subsequent memory effects and dual-attention theory. *Neurobiology of Learning and Memory, 91,* 139–154.

Van Dijk, K. R., Hedden, T., Venkataraman, A., Evans, K. C., Lazar, S. W., & Buckner, R. L. (2010). Intrinsic functional connectivity as a tool for human connectomics: Theory, properties, and optimization. *Journal of Neurophysiology, 103,* 297–321.

Vannini, P., Hedden, T., Huijbers, W., Ward, A. M., Johnson, K. A., & Sperling, R. A. (in press). The ups and downs of the posteromedial cortex: Age- and amyloid-related functional alterations of the encoding/retrieval flip in cognitively normal older adults. *Cerebral Cortex*.

Vannini, P., O'Brien, J., O'Keefe, K., Pihlajamaki, M., Laviolette, P., & Sperling, R. A. (2011). What goes down must come up: Role of the posteromedial cortices in encoding and retrieval. *Cerebral Cortex, 21,* 22–34.

Vilberg, K. L., & Rugg, M. D. (2007). Dissociation of the neural correlates of recognition memory according to familiarity, recollection, and amount of recollected information. *Neuropsychologia, 45,* 2216–2225.

Wagner, A. D., Shannon, B. J., Kahn, I., & Buckner, R. L. (2005). Parietal lobe contributions to episodic memory retrieval. *Trends in Cognitive Sciences, 9,* 445–453.

Wang, L., Zang, Y., He, Y., Liang, M., Zhang, X., Tian, L., et al. (2006). Changes in hippocampal connectivity in the early stages of Alzheimer's disease: Evidence from resting state fMRI. *Neuroimage, 31,* 496–504.

Ward, A. M., Schultz, A. P., Huijbers, W., van Dijk, R. A., Hedden, T., & Sperling, R. A. (in press). Resting-state default mode network connectivity in the medial temporal lobe is distinct from hippocampal regions supporting successful memory formation. *Human Brain Mapping*.

Weissman, D. H., Roberts, K. C., Visscher, K. M., & Woldorff, M. G. (2006). The neural bases of momentary lapses in attention. *Nature Neuroscience, 9,* 971–978.

Yeo, B. T., Krienen, F. M., Sepulcre, J., Sabuncu, M. R., Lashkari, D., Hollinshead, M., et al. (2011). The organization of the human cerebral cortex estimated by intrinsic functional connectivity. *Journal of Neurophysiology, 106,* 1125–1165.